

Article

Analysis of the Correlation between Shielding Material Blending Characteristics and Porosity for Radiation Shielding Films

Seon-Chil Kim ¹ and Sung-Hyoun Cho ^{2,*} 

¹ Department of Biomedical Engineering, School of Medicine, Keimyung University 1095 Dalgubel-daero, Daegu 42601, Korea; rontgen7@gmail.com

² Department of Physical Therapy, Nambu University, Gwangsan-gu, Gwangju 62271, Korea

* Correspondence: geriatricpt1@gmail.com; Tel.: +82-62-970-0232; Fax: +82-62-970-0492

Received: 20 March 2019; Accepted: 24 April 2019; Published: 28 April 2019



Abstract: The most important factors in the manufacture of shielded sheets are shielding ratio, light weight, and tensile strength. The base material should provide a light-shielding film with strong physical shock resistance, while maintaining the shielding ratio of lead. Therefore, we studied the correlation between the porosity during the mixing process and the maintenance of the shielding film characteristics. Changes in the shielding ratio can be predicted according to the properties of materials such as polymeric silicon and tungsten oxide. Further, their tensile strength and porosity may change depending on the content of the material. Experiments were carried out for each substance based on the shielding ratio with respect to the processing conditions. For a shielding film using barium sulfate (BaSO_4) and polymeric silicon, increasing the porosity by the removal of air in the same manufacturing process resulted in a tensile strength of 6.4 MPa at 22% porosity. For tungsten oxide (WO_3), the tensile strength was 10.5 MPa at a porosity of 12%, and for a 0.6 mm sample, the shielding performance was very similar to 0.21 mm of Pb. The porosity during the manufacturing process affected the tensile strength and shielding performance, which were significantly different for each shielding material.

Keywords: radiation protection; radioactive material; X-ray; radiation dose; shielding film

1. Introduction

Medical professionals have been attempting to shield redundant medical radiation facilities. Currently, researchers are developing medical radiation shielding products using new materials that can substitute lead, which is heavy, causes human poisoning, and requires the processing of hazardous waste [1–3]. Bismuth, tungsten, barium, tin, cerium, and antimony are mainly used as shielding materials instead of lead [4]. Because it is desirable to process the material into a thin film, a base material with excellent flexibility is preferred. Currently, a combination of lead and rubber is most frequently used. Heat treatment methods are often used to mix rubber and lead powder [5]. When blending a shielding substance in the manufacturing process, it is difficult to disperse molecules and maintain a homogeneous dispersion. Therefore, there can be problems in the reproducibility of the shielding performance of a manufactured radiation shielding film (RSF). However, the surface hardness and tensile strength of RSFs are typically excellent [6,7].

Base materials of shielding products are polymer resins such as silicone resin or a vinyl chloride resin. These resins can consistently maintain the shielding performance of an RSF, its flexibility, and the tensile strength of the material. When a radiation-shielding substance such as tungsten oxide (WO_3) is blended in, it confers the properties of the radiation-shielding material on the polymer resin,

owing to its outstanding processability and overall safety when used as a base polymer with high hydrophobicity [8,9]. However, problems arising during the compounding process may affect the thickness, strength, and flexibility of the material, resulting in mass-production problems [10]. The strength and hardness (mechanical properties) of the RSF generated in these “environmentally friendly shielding material and polymeric silicon” blending processes are very important for commercialization.

Porosity has a direct relationship with the change in the mechanical properties of the RSF during the “shielding material and polymer resin” blending and mold fabrication processes. Porosity is the percentage void space of the total volume of fillers and granules [11,12]. This is a very important condition for determining the shielding ratio in the RSF fabrication process. The manufacturing method should be upgraded by lowering the thickness and improving the shielding ability, rather than increasing the amount of material.

A laminate processing method evenly disperses particles or, when repeated, fabricates multilayered, multi-gate structures [13–15]. This method of production uses an empirical manufacturing approach rather than a quantitative one. However, there are no specific studies on the quantitative effect of the mixing ratio of the materials, on their porosity, tensile strength, or shielding performance. In particular, there is no general study on the porosity, thickness, shielding performance, and tensile strength of the RSF produced by combining bismuth oxide (Bi_2O_3), tungsten oxide (WO_3), and barium sulfate (BaSO_4), which are the most commonly used shielding materials with polymer resins. There is also no known difference in the final RSF product.

In light of the above, we quantitatively analyzed the effects of environmentally-friendly shielding materials such as Bi_2O_3 , WO_3 , and BaSO_4 on the same polymeric silicone resin, specifically with regard to differences in formulation ratio, porosity, tensile strength, and shielding performance. First, the porosity was observed with an electron microscope capable of magnifying the pores, and influence factors were summarized using formulas. The tensile strength and shielding performance were tested based on the thickness of the RSF and compared with the lead equivalent of shielding performance. We thus aimed to understand the bonding properties between the polymeric resin and the base material, and to quantitatively demonstrate the correlation between the porosity and mechanical properties of the RSF, as well as the shielding ratio during the manufacturing process.

2. Materials and Methods

When a polymer resin is used to make an RSF, the ratio of the shielding material is increased to improve the shielding performance. When the shielding material capacitance is increased to the same base capacitance, the shielding density increases, and the shielding performance improves. However, excessive proportions lower the density of the resin and weaken the tear resistance, which affects the tensile strength and thickness.

During composition, the density is affected by the particle packing and porosity of the composing material. Therefore, the bulk density (D_B) includes air gaps. The true density (D_T) is the mass per unit volume of the shielding material, and it indicates the volume excluding air gaps. To increase the shielding effect, the true density must be increased. However, owing to the difficulty in the manufacturing process, the ratio cannot be provided identically. Therefore, it is calculated using the composition ratio of the shielding material. Porosity can thus be calculated using Equation (1):

$$\text{Porosity (\%)} = \left(1 - \frac{D_B}{D_T}\right) \times 100 \quad (1)$$

and an accurate shielding sheet can be manufactured by mixing the materials. The D_B and the single shielding material particle density (D_T) of a shielding sheet, which is a base material, can be expressed by Equation (2). They are directly proportional to the porosity.

$$D_B = \frac{W_p}{V_p + V_{air}}, D_T = \frac{W_p + W_m}{V + V_p} \quad (2)$$

where D_B is bulk density; D_T is true density; W_p is the weight of the polymer resin in the shielding sheet; W_m is the shielding material weight; V_p is the volume of shielding material; V is the volume of the shielding sheet; V_{air} is the pore volume. Therefore, the porosity of the RSF is calculated using Equations (1) and (2) and can indirectly estimate the bulk density; that is, it can be obtained using the mass and density of the shielding material. Furthermore, two mechanisms can be involved in the compounding process of the polymer resin and shielding material to reduce the porosity.

The shielding materials used in this experiment were Bi_2O_3 , WO_3 , and BaSO_4 , which were pulverized in a miller roller with spacing of 0.1 mm for 120 min; a micro-scale particle size was achieved. We blended polyethylene at regular intervals, and the mixing roller was maintained at 50 °C. Polyethylene is more effective than conventional rubber for heat treatment because thinner flexible sheets can be manufactured. The elasticity is related to the mixing ratio of the shielding material, and shielding sheets with excellent processability can be manufactured. A ratio of 7:3 is the most effective ratio.

After this process, the shielding mixture underwent an aging process at 50 °C for approximately 12 h. Then we manufactured the RSF through compression, vacuuming, and molding with a hydraulic press for 300 s after defoaming. Defoaming is the adequate removal of air by blending with a plasticizer, antioxidants, lubricants, and antistatic agents for 30 min. The shielding sheet shown in the manufacturing process was evaluated for porosity, tensile strength, and shielding ability using the same base material. Accordingly, the composition ratio of the shielding sheets was set to 65% shielding material (Bi_2O_3 , WO_3 , and BaSO_4) and 35% polyethylene. BaSO_4 occurs as the mineral barite, and is the main commercial source of barium used to prepare materials with barium. Bi_2O_3 is the most industrially important compound of bismuth. It is also used as a raw material for bismuth chemistry. WO_3 powder is a middle stage material obtained during the extraction of tungsten from minerals. The tungsten is treated with an alkali, and WO_3 is obtained, see Table 1.

Table 1. Composition description of studied composite specimens.

Specimens	Polyethylene Resin (Standard)	Shielding Material (Ratio)
BaSO_4	35%	65%
Bi_2O_3	35%	65%
WO_3	35%	65%

BaSO_4 : barium sulfate, Bi_2O_3 : bismuth trioxide, WO_3 : tungsten oxide powder.

Three 60 cm long and 60 cm wide sheets of different thicknesses—0.2, 0.4, and 0.6 mm—were produced. To determine the tensile strength of the fabricated RSF, the mechanical properties were measured using a tensile strength meter (Rheometer, MJU-5, CKIS, USA) equipped with a crosshead moving at a constant speed of 5 mm/min.

The X-ray generator used in this experiment was a Toshiba DK-525 (Toshiba E 7239 X, Japan). An exposure detector and rate meter (192 X, Capintec, Florham Park, NJ, USA) as well as an ion chamber (PM-30, Nuclemed NV, Roeselare, Belgium) were also used. A tube current of 200 mA, irradiation time of 0.1 s, intrinsic filtration fixed at 0.7 mm of the X-ray tube, 1.5 mm of collimator, total filtration of 2.2 mm Al, and additional filters of 5.15 mm Al and 5.91 mm Al were used. The tube voltage was determined according to the clinically most used area. The shielding ratio of the manufactured RSF was calculated by averaging the values for 10 measurements performed under configuration conditions, such as those in Figure 1.

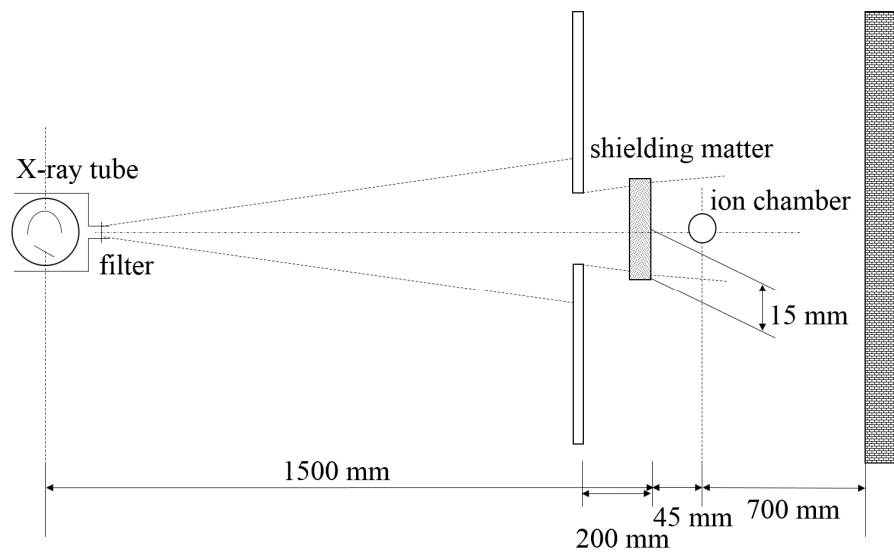


Figure 1. Configuration of the shielding experiment.

Furthermore, the standard lead shielding test for comparative settings was similarly implemented. The medical radiation used in the experiment was confirmed to have energy characteristics as listed in Table 2. The main shielding materials were selected as shown in Table 3 and were the most frequently used materials.

Table 2. Comparison of effective energy to tube voltage.

Tube Voltage (kVp)	Added Filter (mm Al)	Half Value (mm Al)	Effective Energy (keV)
60	5.15	2.96	38.9
80	5.15	3.87	46.3
100	5.15	4.79	52.6
120	5.91	6.04	58.7

Table 3. Characteristic comparison of shielding materials.

Matter	Pb	Ba	Bi	W
Density (g/cm ³)	11.34	3.51	9.78	19.25
Atomic mass (g/mol)	207.2	137.3	208.9	183.8
K—absorption edge (KeV)	88.0	37.4	90.5	69.5
Atomic number	82	56	83	74

3. Results

To improve the shielding performance and tensile strength of the RSF, a defoaming step in the pulverization and mixing process of the shielding material was inserted into the manufacturing process to improve the porosity. To observe the dispersion state of the manufactured RSF, nano-analysis SEM (SUPRA-55VP, Zeiss, Oregon, USA) at 15 kV was used. Figure 2 shows an SEM image of air removal after blending with 25% BaSO₄ and polyethylene for 30 min, and an SEM image for no air removal. As shown in Figure 2, the SEM images of the RSF before and after air removal also showed differences in the flow ratio.

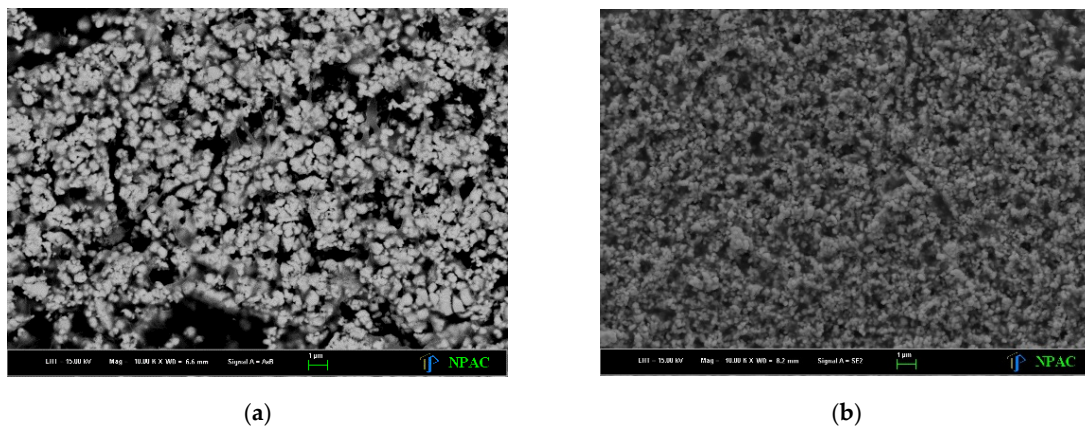


Figure 2. Radiation shielding films (RSF) viewed by SEM, comparing the mixing process with barium sulfate (BaSO_4). (a) Mixing RSF without removing air; (b) mixing RSF with enough air removal.

The density and volume of the materials used were calculated and the results are listed in Table 4. WO_3 with a low porosity due to air removal showed a high tensile strength. When the porosity was higher than 20%, the strength dropped rapidly in the RSF using BaSO_4 . Figure 3 shows the results of the tensile strength of the RSF fabricated by increasing the amount of BaSO_4 added from 250% to 350%, based on 100% silicone resin. As the porosity increased, the tensile strength gradually decreased. Therefore, the importance of air removal through defoaming in the blending process is highlighted.

Table 4. Porosity and tensile strength of shielding films.

Point	Shielding Film (0.6 mm)	BaSO_4	Bi_2O_3	WO_3
	Porosity (%)	+ Silicon Resin		
	Porosity (%)	22	19	12
	Tensile strength (MPa)	6.4	9.2	10.5

BaSO_4 : barium sulfate, Bi_2O_3 : bismuth trioxide, WO_3 : tungsten oxide powder.

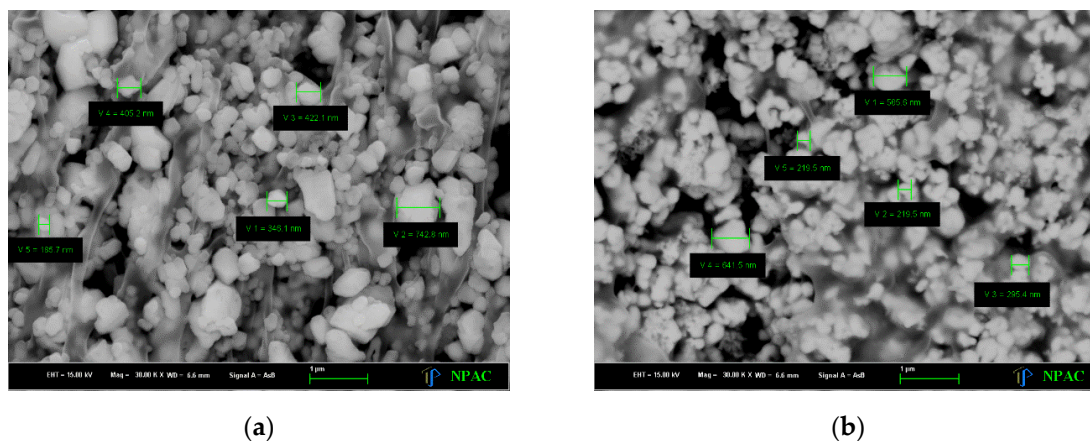


Figure 3. Particle size of shielded film by SEM. (a) Bismuth oxide (Bi_2O_3) and polyethylene compound; (b) tungsten oxide (WO_3) and polyethylene compound.

The result of the tensile strength test performed on the RSF, which was prepared by increasing the amount of BaSO_4 added from 250% to 350% based on 100 units of silicone resin, is shown in Figure 3. The figure is an SEM image obtained by comparing the shielding materials of the RSF. It is a combination of tungsten and bismuth, which is widely used as an eco-friendly material. As shown in Figure 3, there is no significant difference in the appearance of the internal organization. However, a difference in size is shown in the composition of the particles.

The indication is that the bonding state is maintained while the WO₃ maintains the size of micro units in the formulation of a polymer resin. As the pore size decreases, the porosity mostly tends to decrease, and as the porosity decreases, the shielding ratio improves. The shielding performance of the RSF manufactured for each shielding material was conducted using the experimental conditions proposed in this study. For a comparative evaluation of the RSF, the standard lead shielding performance was obtained under the same experimental conditions shown in Table 5.

Table 5. Standard lead penetration dose (unit: mR).

Tube Voltage (kV)	Thickness (mm)					
	None	0.25	0.30	0.35	0.40	0.40
60	15.00	0.10	0.05	0.01	0.01	0.002
80	39.82	2.15	1.52	0.82	0.82	0.04
100	60.04	5.09	3.86	2.81	2.81	1.95
120	80.20	9.26	7.10	5.14	5.14	3.01

The shielding performance of the RSFs made of BaSO₄, Bi₂O₃, and WO₃ are shown in Figure 4; that of the shielding product improved owing to the thicker layer, and it differed in the order of WO₃, Bi₂O₃, and BaSO₄. Particularly, at 0.2 mm, higher energy corresponded to a larger difference in the shielding ratio of the BaSO₄ component. The shielding ratio refers to the degree of shielding performance, which is obtained using the formula $(1 - w/w1) \times 100$, where *w* denotes the case with the shielding material and *w1* denotes the case without the shielding material. When WO₃ was used, it showed an almost stable shielding performance for a thickness of 0.6 mm. Shielding was not always 100%; that is, the material thickness was fixed at three different values, depending on the shielding ratio and the material used. A shielding ratio of 100% for tungsten indicates that 100% shielding is achieved with no penetration at a low energy of 60 kV.

As a result, as shown in the graph, the same shielding tendency is shown by the change in the tube voltage. Figure 4 shows that the shielding ratio decreases with increasing energy. However, the difference in the ratio varies depending on the material owing to the difference in porosity. This difference is low for the low-porosity WO₃ composite and high for the BaSO₄ shield.

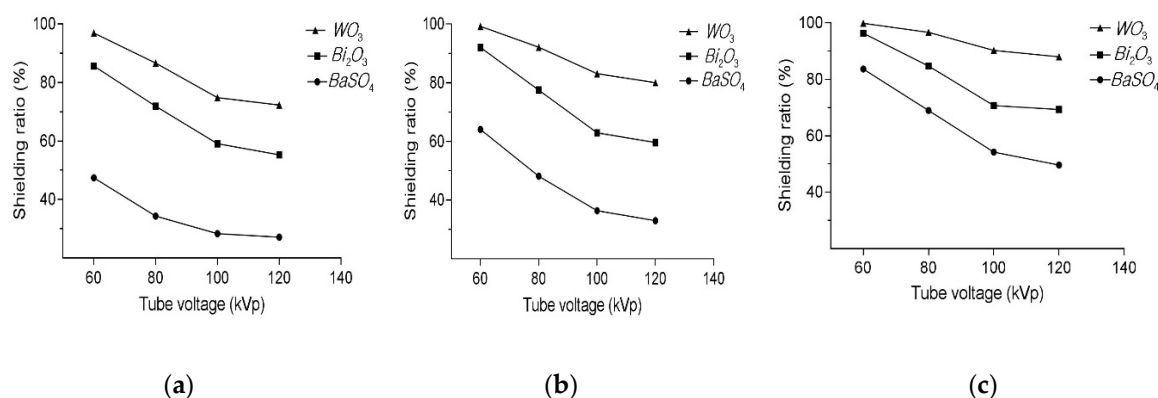


Figure 4. Shielding ability as a function of film thickness. (a) Shielding performance of 0.2 mm shielding films; (b) shielding performance of 0.4 mm shielding films; (c) shielding performance of 0.6 mm shielding films. WO₃: tungsten oxide powder; Bi₂O₃: bismuth trioxide; BaSO₄: barium sulfate.

There was a difference in the individual shielding ability of the RSF manufactured for each material, and the shielding performance also changed with the thickness. As a numerical estimate, it can be expressed by the transmission dose and lead equivalent, as presented in Table 6 [16]. The RSF using BaSO₄—based on the 0.6 mm RSF—corresponds to 0.5 mm Pb of the lead equivalent, 0.4 mm Pb of the Bi₂O₃, and 0.1 mm Pb of the WO₃.

Table 6. Shielding film of penetration dose (unit: mR).

Shielding Film	BaSO ₄	Bi ₂ O ₃	WO ₃
	+Silicon Resin		
Penetration dose (mR)	3.89	2.83	1.02
Lead equivalent (mm Pb)	0.547	0.398	0.121

BaSO₄: barium sulfate, Bi₂O₃: bismuth trioxide, WO₃: tungsten oxide powder. Penetration dose measurements are based on the prepared 0.6 mm sheet (200 mA, 0.1 s, 100 kVp).

The individual shielding ability of the RSF prepared for each material varied, and the shielding performance also depended on the thickness. For numerical estimation, the penetration dose can be measured to show the lead equivalent. Therefore, an RSF using BaSO₄ based on 0.6 mm thickness corresponds to 0.5 mm Pb of lead equivalent, and the RSF using Bi₂O₃ and WO₃ correspond to 0.4 and 0.1 mm Pb, respectively.

It was found that the correlation between the porosity and the shielding ratio showed a decreasing trend, as seen Figure 5. However, as the strength increased, the shielding ratio improved.

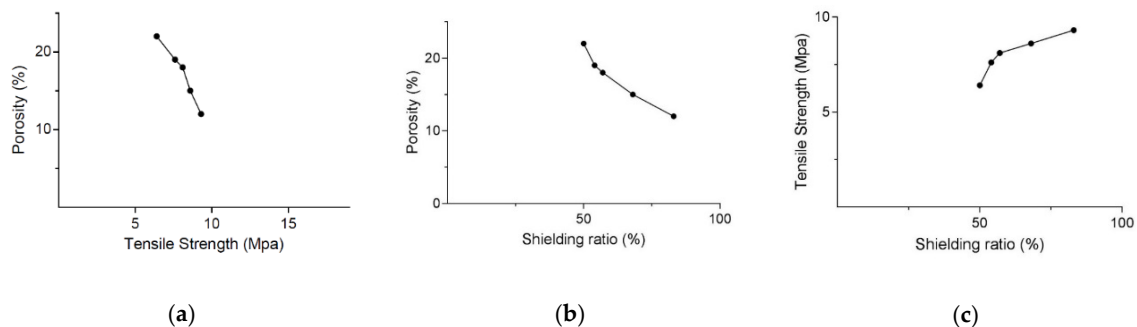


Figure 5. Correlation between porosity, tensile strength, and radiation shielding ratio (barium sulfate (BaSO₄) 6 mm). (a) Comparison of tensile strength and porosity; (b) comparison of shielding performance and porosity; (c) comparison of shielding performance and tensile strength.

4. Discussion

In earlier research, the discovery of environmentally-friendly shielding materials with excellent processability was the primary objective, and the concepts of mass and density were important. Now, they are very important factors for the processability of an RSF. The durability and organization between a shield material and the process technology have been studied [17,18]. For RSFs in the industrial field, an important condition for the safe transfer of contaminated substances after the Fukushima incident in Japan was that the minimum strength should support the weight. The RSF in the medical field is an important factor necessary for medical personnel wear. Radiation shielding has a larger shielding effect for a larger mass of material. However, it is not necessarily proportional to the shielding performance.

As shielding performance is related to material density—and density is the relationship between the volume and the mass—processes such as blending the shielding materials are very important. The basic processing of the RSF was carried out by powdering, mixing, forming, aging, and extruding the material. The manufacturing process that increased the interval density—achieved by lowering the porosity for the removal of primary bubbles in the mixing process and secondary bubbles in the aging process—was very important in this experiment.

In earlier studies, a mechanical method was selected to increase the degree of dispersion and packing of the shielding material [19]. However, we applied the porosity that is suggested in this study because the problem of tensile strength of the RSF after fabrication occurred. Consequently,

the shielding performance could be predicted with the porosity when calculating the bulk density of the RSF.

Therefore, in the RSF manufacturing process, to maintain a light weight, a shielding material such as WO_3 , Bi_2O_3 , tin, or antimony trioxide is pulverized into micro units in a polymer silicone resin rather than excess added powder, to obtain uniform compounding. Bubble removal in the mixing process is also very important. To lower the porosity, the multi-gate method by stepwise dosing according to the particle size was proposed [20–22]. However, bubble removal has a considerable influence on the performance of the RSF.

The porosity during the RSF manufacturing process varies depending on the shielding material and base material. However, generally, it is most stable between 12% and 20%, and the actual value, considering the tensile strength, is estimated to be approximately 15%. For such conditions, the shielding ratio can show an excellent performance of 90% or more. The thickness of the RSF also has a direct correlation with the shielding performance.

If the shielding material is thick, the reason the shielding ratio does not decrease rapidly, owing to an increase in voids, may be a tendency of the radiation to be partially reduced through scattering and absorption in the internal structure of the particles [19,23]. Therefore, the thickness of the RSF should be adjusted to a lightweight standard and should not affect the tensile strength.

Considering the properties of the RSF (the tensile strength, surface hardness, flexibility, and processability), the other characteristics should be considered. Some can be solved with additives, such as plasticizers in the mixing process. However, some need to be further improved. Therefore, important factors in the fabrication of RSFs are the choice of shielding materials, blending with silicone resin, process steps such as molding, and the porosity of the internal structure.

5. Conclusions

We investigated the correlation between the porosity, tensile strength, and shielding performance of an RSF fabricated with BaSO_4 , Bi_2O_3 , and WO_3 blended with polymer silicone resin based on a lightweight and ecological theme. There was no considerable change except for the RSF using BaSO_4 . It was found that a lower porosity corresponded to a higher tensile strength and shielding performance. However, although the shielding ratio of the RSF using Bi_2O_3 was lower than that of WO_3 , there was no considerable difference in porosity. Based on these results, it was confirmed that porosity correlated with the shielding performance of an RSF and its mechanical properties, such as tensile strength.

Author Contributions: Project administration, S.-C.K. and S.-H.C.; performed the experiments and data analysis, S.-C.K. and S.-H.C.; writing—original draft, S.-H.C.; writing—review and S.-C.K. and S.-H.C.; editing

Funding: This work was supported by the National Research Foundation of Korea (NRF) grant funded by the Korea government (MSIT) (No. 2017R1C1B5076499). This study was supported (in part) by research funds from Nambu University, 2019.

Acknowledgments: I would like to thank Editage (www.editage.co.kr) for polishing the language in the manuscript.

Conflicts of Interest: The authors declare no conflict of interest.

References

1. Yue, K.; Luo, W.; Dong, X.; Wang, C.; Wu, G.; Jiang, M.; Zha, Y. A new lead-free radiation shielding material for radiotherapy. *Radiat. Prot. Dosim.* **2009**, *133*, 256–260. [[CrossRef](#)] [[PubMed](#)]
2. McCaffrey, J.P.; Shen, H.; Downton, B.; Mainegra-Hing, E. Radiation attenuation by lead and nonlead materials used in radiation shielding garments. *Med. Phys.* **2007**, *34*, 530–537. [[CrossRef](#)]
3. Stam, W.; Pillay, M. Inspection of lead aprons: a practical rejection model. *Health Phys.* **2008**, *95*, 133–136. [[CrossRef](#)]
4. Szajerski, P.; Zaborski, M.; Bem, H.; Baryn, W.; Kusiak, E. Optimization of the heavy metal (Bi-W-Gd-Sb) concentrations in the elastomeric shields for computer tomography (CT). *J. Radioanal. Nucl. Chem.* **2014**, *300*, 385–391. [[CrossRef](#)]

5. Asai, S.; Miyoshi, K.; Saito, K. Modification of a porous sheet (MAPS) for the high-performance solid-phase extraction of trace and ultratrace elements by radiation-induced graft polymerization. *Anal. Sci.* **2010**, *26*, 649–658. [[CrossRef](#)] [[PubMed](#)]
6. Kim, S.C.; Choi, J.R.; Jeon, B.K. Physical analysis of the shielding capacity for a lightweight apron designed for shielding low intensity scattering X-rays. *Sci. Rep.* **2016**, *6*, 27721. [[CrossRef](#)]
7. Yang, J.P.; Chen, Z.K.; Yang, G.; Fu, S.Y.; Ye, L. Simultaneous improvements in the cryogenic tensile strength, ductility and impact strength of epoxy resins by a hyperbranched polymer. *Polymer* **2008**, *49*, 3168–3175. [[CrossRef](#)]
8. Yin, Y.L.; Prud'homme, R.K.; Stanley, F. *Polyelectrolyte Gels*; Harland, R.S., Prud'homme, R.K., Eds.; ACS Symposium Series 480; ACS: Washington, DC, USA, 1992; pp. 91–113.
9. Gwaily, S.E.; Hassan, H.H.; Badawy, M.M.; Madani, M. Study of electrophysical characteristics of lead-natural rubber composites as radiation shields. *Polym. Compos.* **2002**, *23*, 1068–1075. [[CrossRef](#)]
10. Nambiar, S.; Osei, E.; Yeow, J.T.W. Polymer nanocomposite-based shielding against diagnostic X-rays. *J. Appl. Polym. Sci.* **2013**, *127*, 4939–4946. [[CrossRef](#)]
11. Min, T.B.; Cho, I.S.; Lee, H.S. Fundamental study on the strength development of cement paste using hardening accelerator and high-early-strength cement. *J. Korea Inst. Build. Construct.* **2013**, *13*, 407–415. [[CrossRef](#)]
12. Kim, S.C.; Lee, H.K.; Cho, J.H. Analysis of low-dose radiation shield effectiveness of multi-gate polymeric sheets. *Radiat. Eff. Defect Solids* **2014**, *169*, 584–591. [[CrossRef](#)]
13. Kinsella, J.M.; Jimenez, R.E.; Karmali, P.P.; Rush, A.M.; Kotamraju, V.R.; Gianneschi, N.C.; Ruoslahti, E.; Stupack, D.; Sailor, M.J. X-ray computed tomography imaging of breast cancer by using targeted peptide-labeled bismuth sulfide nanoparticles. *Angew. Chem. Int. Ed. Engl.* **2011**, *50*, 12308–12311. [[CrossRef](#)]
14. Jones, A.K.; Pasciak, A.S.; Wagner, L.K. Impact of using scatter-mimicking beams instead of standard beams to measure penetration when assessing the protective value of radiation-protective garments. *Med. Phys.* **2018**, *45*, 1071–1079. [[CrossRef](#)]
15. Xiao, H.; Lu, Y.; Wang, M.; Qin, X.; Zhao, W.; Luan, J. Effect of gamma-irradiation on the mechanical properties of polyacrylonitrile-based carbon fiber. *Carbon* **2013**, *52*, 427–439. [[CrossRef](#)]
16. National Committee on Radiation Protection. *Structural Shielding Design for Medical X-ray Imaging Facilities*; NCRP: Oak Brook, IL, USA, 2004; pp. 10–20.
17. Evcin, O.; Evcin, A.; Bezir, N.C.; Akkurt, I.; Gunoglu, K.; Ersoy, B. Production of barite and boroncarbide doped radiation shielding polymer composite panels. *Acta Phys. Pol. A* **2017**, *132*, 1145–1148. [[CrossRef](#)]
18. Xu, S.; Bourham, M.; Rabiei, A. A novel ultra-light structure for radiation shielding. *Mater. Des.* **2010**, *31*, 2140–2146. [[CrossRef](#)]
19. Li, R.; Gu, Y.; Yang, Z.; Li, M.; Hou, Y.; Zhang, Z. Gamma ray shielding property, shielding mechanism and predicting model of continuous basalt fiber reinforced polymer matrix composite containing functional filler. *Mater. Des.* **2017**, *124*, 121–130. [[CrossRef](#)]
20. Ray, S.S.; Okamoto, M. Polymer/layered silicate nanocomposites: A review from preparation to processing. *Prog. Polym. Sci.* **2013**, *28*, 1539–1641.
21. Wang, T.; Wang, M.; Zhang, Z.; Ge, X.; Fang, Y. Grafting of polymers from clay nanoparticles via high-dose gamma-ray irradiation. *Mater. Lett.* **2007**, *61*, 3723–3727. [[CrossRef](#)]
22. Shah, D.; Maiti, P.; Jiang, D.D.; Batt, C.A. Effect of nanoparticle mobility on toughness of polymer nanocomposites. *Adv. Mater.* **2005**, *17*, 525–528. [[CrossRef](#)]
23. Buyuk, B.; Tugrul, A.B. Comparison of lead and WC-Co materials against gamma irradiation. *Acta Phys. Pol. A* **2014**, *125*, 423–425. [[CrossRef](#)]

